Dyes and Pigments 105 (2014) 180–191

Contents lists available at ScienceDirect

Dyes and Pigments

journal homepage: www.elsevier.com/locate/dyepig

A series of 3D isomorphous lanthanide coordination polymers based on flexible dicarboxylate ligand: Synthesis, structure, characterization, and properties

Lirong Yang*, Liu Liu, Lanzhi Wu, Huaimin Zhang, Shuang Song

Henan Key Laboratory of Polyoxometalate, Institute of Molecule and Crystal Engineering, College of Chemistry and Chemical Engineering, Henan University, Jinming Street, Kaifeng 475004, PR China

ARTICLE INFO

Article history:
Received 11 December 2013
Received in revised form
28 January 2014
Accepted 31 January 2014
Available online 16 February 2014

Keywords:
Lanthanide–organic framework
Coordination polymer
Synthesis
Characterization
Magnetic properties
Luminescent properties

ABSTRACT

Seven lanthanide coordination polymers, namely, $\{[Ln(BDOA)_{1.5}(H_2O)]\cdot H_2O\}_n$ (Ln = Ce(**I**), Pr(**II**), Nd(**III**), Sm(**IV**), Eu(**V**), Gd(**VI**), and Tb(**VII**), H_2BDOA = benzene-1,4-dioxydiacetic acid), have been synthesized through hydrothermal reactions of lanthanide nitrate with H_2BDOA ligands and characterized by elemental analysis, infrared spectroscopy and single crystal X-ray diffraction. Findings indicate that **I**–**VI** are isomorphous and isostructural, containing the subunit of cavate 10-membered cages ($Ln_2O_2(OCO)_2$), while **VII** possesses the subunit of cavate 14-membered cages ($Tb_2(OCO)_4$), based on which to assemble into three-dimensional porous architectures *via* $BDOA^{2-}$ ligands, hydrogen bonds and C–H···π interactions. **I** and **III** present antiferromagnetic behaviors and lanthanide contraction effect exists in **I**–**VI**. Luminescent studies suggest the typical intense emissions of Ln(III) ions occur in the visible region and therefore the coordination polymers display good selectivity towards some certain metal ions such as Ca^{2+} and Cd^{2+}, showing promising potential as selective luminescent probes of these metal ions.

1. Introduction

Metal–organic frameworks based on lanthanide-containing coordination polymers have provoked great interest owing to the combination of organic and inorganic fragments that may generate a large number of intriguing topological structures [1–3]. Particularly, lanthanide-containing coordination polymers allow that rational design strategies for constructing porous materials with high surface areas, predictable structures, tunable pore sizes and may find potentially industrial applications in gas storage and separation, adsorption catalysis, guest exchange, ion exchange, molecular recognition, molecular magnetism, nonlinear optics and luminescent, etc [4–14]. In addition, lanthanide ions own larger radius and higher affinity for hard donor centers and ligands with oxygen or hybrid oxygen–nitrogen atoms, which are in favor of the construction of coordination polymers [15–18]. What's more, lanthanide ions with special luminescent and magnetic properties resulting from 4f electrons, which illustrated the coordination polymers are intriguing and remarkably suitable for the development of optical devices and magnetic device as well as probes for chemical species and magnetic targeting drug system [19–30]. Naturally, multidentate organic ligands like polycarboxylic acids are recommended as the linkers of metal ions to polymerize into extended open frameworks, because these ligands may potentially provide various coordination modes and favor the construction of multi-dimensional coordination polymers [31–37]. Specifically, flexible linker benzene-1,4-dioxyacetic acid (H_2BDOA) contains carboxylate oxygen atoms and ether oxygen atoms and exhibits several interesting characteristics: (i) it can be deprotonated to generate $HBDOA^-$ and $BDOA^{2-}$ by controlling the pH values carefully, which allows it to display various acidity-dependant coordination modes; (ii) chelating and bridging coordination through carboxy oxygen and ether oxygen atoms benefit its versatile bonding fashions; (iii) it features as a combination of rigidity (benzene ring) and flexibility (pendant arms) which is favorable for the construction of multi-dimensional coordination polymers [38–43]; (iv) the benzene ring in $BDOA^{2-}$ ligand may transfer the energy to the Ln(III) centers to enhance the luminescence efficiently [44–47]; (v) carboxyl groups in $BDOA^{2-}$ ligand can provide the short exchange pathway to achieve magnetic exchange between the Ln(III) centers [48–51]. Therefore, acting as the flexible carboxylate linkers,

* Corresponding author.
E-mail addresses: lirongyang@henu.edu.cn, lirongyang@163.com (L. Yang).

http://dx.doi.org/10.1016/j.dyepig.2014.01.032
0143-7208/

$BDOA^{2-}$ ligand may be a potential candidate to fabricate multi-functional lanthanide-containing coordination polymers.

Following our ongoing efforts towards the synthesis and isolation of lanthanide-containing coordination polymers [52–55]. In this work, we describe the synthesis, structures, thermal analysis and luminescent properties of seven 3D coordination polymers obtained from the self-assembly of bridging ligands benzene-1,4-dioxyacetic acid and Ln(III) ions, which are formulated as $\{[Ln(BDOA)_{1.5}(H_2O)]\cdot H_2O\}_n$ (Ln = Ce(**I**), Pr(**II**), Nd(**III**), Sm(**IV**), Eu(**V**), Gd(**VI**), and Tb(**VII**)). The coordination polymers reported herein, are expounding the structure comparison of the coordination polymers and lanthanide contraction effect on their structures.

2. Experimental section

2.1. Materials and physical measurements

All chemicals were commercially purchased and used without further purification. Elemental analyses (C, H, and N) were performed with a Perkin–Elmer 240 CHN Elemental Analyzer. IR spectra in the range of 400–4000 cm^{-1} were recorded with an AVATAR 360 FT-IR spectrometer (KBr pellets were used). The crystal structure was determined with a Bruker Smart CCD X-ray single-crystal diffractometer. TG analysis was conducted with a Perkin–Elmer TGA7 instrument in flowing N_2 at a heating rate of 10 °C min^{-1}. Excitation and emission spectra were obtained with an F-7000 FL spectrofluorometer at room temperature. Magnetic susceptibility measurements were conducted with a Quantum Design MPMS-5 magnetometer in the temperature range of 2.0–300.0 K.

2.2. Synthesis of the coordination polymers *I–VII*

2.2.1. Synthesis of the ligand of benzene-1,4-dioxydiacetic acid (1,4-H_2BDOA)

A mixture of Chloroacetic acid (8 mmol) and 1,4-Benzenediol (2 mmol) was dissolved in water (20 mL) and stirred at 80 °C for 2 h. The pH value was maintained at 11 by dropwise adding of sodium hydroxide solution (1.0 mol L^{-1}). Then the reaction mixture was cooled to room temperature and was adjusted to pH ≈ 3 with HCl (1.0 mol L^{-1}), simultaneously. The brown powder of benzene-1,4-dioxydiacetic acid (1,4-H_2BDOA) formed immediately, which was isolated by filtration and washed with distilled water. The product was dried at 50 °C for 24 h. Yield: 85.40%. Elemental analysis calculated for $C_{10}H_{10}O_6$ (226.05): C 53.10, H 4.46; Found: C 53.45, H 4.26. MS *m/z*: 226.21. IR data (KBr pellet, cm^{-1}): 3415(br), 1753(s), 1633(w), 1508(m), 1428(w), 1385(w), 1322(w), 1289(w), 1227(s), 1091(s), 992(w), 993(w), 889(w), 824(w), 799(w), 665(m), 555(w).

2.2.2. Synthesis of the coordination polymers $\{[Ce(BDOA)_{1.5}(H_2O)]\cdot H_2O\}_n$ (*I*)

$\{[Ce(BDOA)_{1.5}(H_2O)]\cdot H_2O\}_n$ (I) was synthesized from the reaction mixture of benzene-1,4-dioxyacetic acid and cerium nitrate at a molar ratio of 1:2 (0.1 mmol:0.2 mmol) in 10 mL distilled water with a drop of DMF. The resultant mixture was homogenized by stirring for 20 min at ambient temperature and then transferred into 20 mL Teflon-lined stainless steel autoclave under autogenous pressure at 180 °C for 4 days and then cooled to room temperature at a rate of 5 °C/h. After filtration, the product was washed with distilled water and then dried to afford yellowish block-shaped crystals suitable for X-ray diffraction analysis. Elemental analysis

Table 1
Summary of crystallographic data for coordination polymers **I–VII**.

Data	I	II	III	IV	V	VI	VII
Empirical formula	$C_{15}H_{16}O_{11}Ce$	$C_{15}H_{16}O_{11}Pr$	$C_{15}H_{16}O_{11}Nd$	$C_{15}H_{16}O_{11}Sm$	$C_{15}H_{16}O_{11}Eu$	$C_{15}H_{16}O_{11}Gd$	$C_{15}H_{16}O_{11}Tb$
Formula weight	512.40	513.19	516.52	522.63	524.24	529.53	531.20
Temperature/K	296(2)	296(2)	296(2)	296(2)	296(2)	296(2)	296(2)
Wavelength/Å	0.71073	0.71073	0.71073	0.71073	0.71073	0.71073	0.71073
Crystal system	Monoclinic	Monoclinic	Monoclinic	Monoclinic	Monoclinic	Monoclinic	Monoclinic
Space group	*P*21/*c*	*P*21/*c*	*P*21/*c*	*P*21/*c*	*P*21/*c*	*P*21/c	*P*21/*c*
a/Å	12.1598(11)	12.1268(7)	12.1306(4)	12.1121(10)	12.0782(3)	12.0700(9)	12.0280(4)
b/Å	16.8436(15)	16.7341(10)	16.6998(6)	16.6262(13)	16.5903(5)	16.6000(12)	16.7363(6)
c/Å	8.9322(8)	8.9193(5)	8.9406(3)	8.9174(7)	8.8853(2)	8.8690(6)	8.5719(3)
α/(°)	90	90	90	90	90	90	90
β/(°)	109.0400(10)	109.1840(10)	109.281(1)	109.361(10)	109.33	109.3410(10)	108.932(1)
γ/(°)	90	90	90	90	90	90	90
Z	4	4	4	4	4	4	4
Density (calculated)	1.968 Mg/m^3	1.994 Mg/m^3	2.007 Mg/m^3	2.049 Mg/m^3	2.073 Mg/m^3	2.098 Mg/m^3	2.117 Mg/m^3
F(000)	1008	1012	1016	1024	1028	1032.0	1036
Crystal size/mm^3	0.43 × 0.17 × 0.08	0.33 × 0.25 × 0.19	0.54 × 0.36 × 0.14	0.49 × 0.22 × 0.13	0.41 × 0.21 × 0.20	0.21 × 0.19 × 0.18	0.45 × 0.23 × 0.19
θ range for data collection/(°)	1.77–25.00	1.78–25.00	2.16–25.00	1.78–25.00	1.79–24.99	1.79–25.00	1.79–24.99
Limiting indices	$-14 \le h \le 14$, $-20 \le k \le 18$, $-10 \le l \le 9$	$-14 \le h \le 10$, $-19 \le k \le 19$, $-9 \le l \le 10$	$-14 \le h \le 8$, $-19 \le k \le 18$, $-10 \le l \le 10$	$-14 \le h \le 14$, $-16 \le k \le 9$, $10 \le l \le 10$	$-11 \le h \le 14$, $-19 \le k \le 17$, $-10 \le l \le 7$	$-14 \le h \le 14$, $-19 \le k \le 19$, $-9 \le l \le 10$	$-13 \le h \le 14$, $-19 \le k \le 11$, $-10 \le l \le 10$
Reflections collected/ unique	11101/3048 [$R_{(int)} = 0.0317$]	10976/3018 [$R_{(int)} = 0.0192$]	10990/3015 [$R_{(int)} = 0.0212$]	10800/2992 [$R_{(int)} = 0.0222$]	10749/2961 [$R_{(int)} = 0.0168$]	10598/2952 [$R_{(int)} = 0.0186$]	9464/2939 [$R_{(int)} = 0.0149$]
Refinement method	Full-matrix least-squares on F^2						
Data/restraints/ parameters	3048/0/244	3018/0/244	3015/0/244	2992/0/244	2961/0/244	2952/0/244	2939/0/244
Goodness-of-fiton F^2	1.067	1.081	1.048	1.075	1.112	1.111	1.132
Volume/$Å^3$	1729.4(3)	1709.49(17)	1709.6(1)	1694.2(2)	1680.08(8)	1676.7(2)	1666.49(1)
Final Rindices [$I > 2\sigma(I)$]	$R_1 = 0.0201$, $wR_2 = 0.0501$	$R_1 = 0.0174$, $wR_2 = 0.0425$	$R_1 = 0.0171$, $wR_2 = 0.0424$	$R_1 = 0.0174$, $wR_2 = 0.0458$	$R_1 = 0.0156$, $wR_2 = 0.0418$	$R_1 = 0.0180$, $wR_2 = 0.0485$	$R_1 = 0.0170$, $wR_2 = 0.0440$
Rindices (alldata)	$R_1 = 0.0238$, $wR_2 = 0.0518$	$R_1 = 0.0194$, $wR_2 = 0.0433$	$R_1 = 0.0189$, $wR_2 = 0.0432$	$R_1 = 0.0188$, $wR_2 = 0.0464$	$R_1 = 0.0171$, $wR_2 = 0.0423$	$R_1 = 0.0193$, $wR_2 = 0.0491$	$R_1 = 0.0182$, $wR_2 = 0.0445$
Largest diff. peak and hole/(e $Å^{-3}$)	0.399 and −0.441	0.347 and −0.442	0.350 and −0.479	0.72 and −0.48	0.64 and −0.58	0.790 and −0.644	0.57 and −0.59

Table 2
Selected bond lengths (Å) and bond angles (°) for the coordination polymers **I**–**VII**.

Bond long (Å)					
I					
Ce(1)–O(6)	2.4211(18)	Ce(1)–O(5)	2.510(2)	Ce(1)–O(1)	2.490(2)
Ce(1)–O(8)	2.4379(19)	Ce(1)–O(1W)	2.532(2)	Ce(1)–O(3)	2.7074(18)
Ce(1)–O(2)	2.483(2)	Ce(1)–O(7)	2.582(2)	Ce(1)–O(8A)	2.784(2)
II					
Pr(1)–O(6)	2.3992(17)	Pr(1)–O(1W)	2.507(2)	Pr(1)–O(1)	2.4700(18)
Pr(1)–O(7)	2.4126(18)	Pr(1)–O(8)	2.5579(19)	Pr(1)–O(7)	2.764(2)
Pr(1)–O(2)	2.4637(18)	Pr(1)–O(3)	2.6826(17)	Pr(1)–O(5)	2.4842(18)
III					
Nd(1)–O(3)	2.6716(17)	Nd(1)–O(1W)	2.496(2)	Nd(1)–O(2)	2.4608(18)
Nd(1)–O(5)	2.4712(18)	Nd(1)–O(1)	2.4610(17)	Nd(1)–O(7)	2.7529(19)
Nd(1)–O(8)	2.5471(18)	Nd(1)–O(6)	2.3927(17)	Nd(1)–O(7a)	2.3990(18)
IV					
Sm(1)–O(7)	2.362(2)	Sm(1)–O(1W)	2.456(2)	Sm(1)–O(1)	2.4378(19)
Sm(1)–O(2)	2.3627(17)	Sm(1)–O(8)	2.510(2)	Sm(1)–O(7)	2.779(2)
Sm(1)–O(5)	2.4328(19)	Sm(1)–O(4)	2.6476(17)	Sm(1)–O(6)	2.4434(19)
V					
Eu(1)–O(8)	2.3429(19)	Eu(1)–O(2W)	2.441(2)	Eu(1)–O(5)	2.4190(19)
Eu(1)–O(6)	2.3455(17)	Eu(1)–O(7)	2.4855(19)	Eu(1)–O(8)	2.803(2)
Eu(1)–O(1)	2.4172(19)	Eu(1)–O(3)	2.6323(17)	Eu(1)–O(2)	2.4297(18)
VI					
Gd(1)–O(2)	2.326(2)	Gd(1)–O(1W)	2.430(2)	Gd(1)–O(9)	2.410(2)
Gd(1)–O(4)	2.3373(19)	Gd(1)–O(3)	2.470(2)	Gd(1)–O(2a)	2.836(3)
Gd(1)–O(5)	2.401(2)	Gd(1)–O(7)	2.6223(19)	Gd(1)–O(8)	2.417(2)
VII					
Tb(1)–O(7)	2.281(3)	Tb(1)–O(1)	2.396(2)	Tb(1)–O(2)	2.393(2)
Tb(1)–O(6)	2.312(2)	Tb(1)–O(8)	2.412(2)	Tb(1)–O(3)	2.6155(19)
Tb(1)–O(5)	2.375(2)	Tb(1)–O(1W)	2.417(2)		
Bond angle (°)					
I					
O(6)–Ce(1)–O(8)	70.43(7)	O(2)–Ce(1)–O(7)	129.24(7)	O(8)–Ce(1)–O(7)	120.19(6)
O(6)–Ce(1)–O(2)	73.66(7)	O(2)–Ce(1)–O(3)	70.62(6)	O(8)–Ce(1)–O(3)	149.34(6)
O(6)–Ce(1)–O(1)	138.49(7)	O(2)–Ce(1)–O(8)	138.77(6)	O(8)–Ce(1)–O(8)	74.35(7)
O(6)–Ce(1)–O(5)	132.89(6)	O(1)–Ce(1)–O(5)	72.30(6)	O(2)–Ce(1)–O(1)	114.07(7)
O(6)–Ce(1)–O(1W)	139.46(7)	O(1)–Ce(1)–O(1W)	74.10(8)	O(2)–Ce(1)–O(5)	134.81(7)
O(6)–Ce(1)–O(7)	73.05(7)	O(1)–Ce(1)–O(7)	71.77(7)	O(2)–Ce(1)–O(1W)	69.48(7)
O(6)–Ce(1)–O(3)	88.48(6)	O(1)–Ce(1)–O(3)	59.77(6)	O(1W)–Ce(1)–N(7)	145.65(8)
O(6)–Ce(1)–O(8)	66.84(6)	O(1)–Ce(1)–N(8)	103.37(7)	O(1W)–Ce(1)–N(3)	94.68(7)
O(8)–Ce(1)–O(2)	81.94(7)	O(5)–Ce(1)–N(1W)	75.00(7)	O(1W)–Ce(1)–O(8)	140.75(7)
O(8)–Ce(1)–O(1)	148.61(6)	O(5)–Ce(1)–N(7)	95.77(7)	O(7)–Ce(1)–O(3)	71.29(6)
O(8)–Ce(1)–O(5)	77.44(7)	O(5)–Ce(1)–N(3)	132.05(6)	O(7)–Ce(1)–O(8)	48.04(6)
O(8)–Ce(1)–O(1W)	88.05(8)	O(5)–Ce(1)–N(8)	71.97(6)		
II					
O(6)–Pr(1)–O(2)	138.52(7)	O(5)–Pr(1)–O(8)	95.70(7)	O(1)–Pr(1)–O(1W)	69.42(6)
O(7)–Pr(1)–O(2)	148.39(6)	O(1W)–Pr(1)–O(8)	145.90(8)	O(5)–Pr(1)–O(1W)	70.15(7)
O(6)–Pr(1)–O(1)	73.36(6)	O(6)–Pr(1)–O(3)	87.88(6)	O(6)–Pr(1)–O(8)	73.12(7)
O(7)–Pr(1)–O(1)	82.04(6)	O(7)–Pr(1)–O(3)	149.18(6)	O(7)–Pr(1)–O(8)	119.99(6)
O(2)–Pr(1)–O(1)	114.18(7)	O(2)–Pr(1)–O(3)	60.23(6)	O(2)–Pr(1)–O(8)	71.89(7)
O(6)–Pr(1)–O(5)	133.05(6)	O(1)–Pr(1)–O(3)	70.49(6)	O(1)–Pr(1)–O(8)	129.32(7)
O(7)–Pr(1)–O(5)	77.18(6)	O(5)–Pr(1)–O(3)	132.54(6)	O(1)–Pr(1)–O(7)	138.56(6)
O(2)–Pr(1)–O(5)	72.31(6)	O(1W)–Pr(1)–O(3)	95.03(7)	O(5)–Pr(1)–O(7)	71.74(6)
O(1)–Pr(1)–O(5)	134.83(7)	O(8)–Pr(1)–O(3)	71.38(6)	O(1W)–Pr(1)–O(7)	140.49(6)
O(6)–Pr(1)–O(1W)	139.15(7)	O(6)–Pr(1)–O(7)	67.09(6)	O(8)–Pr(1)–O(7)	48.32(6)
O(7)–Pr(1)–O(1W)	87.90(8)	O(7)–Pr(1)–O(7)	73.83(7)	O(3)–Pr(1)–O(7)	118.62(6)
O(2)–Pr(1)–O(1W)	74.23(8)	O(2)–Pr(1)–O(7)	103.65(7)		
III					
O(3)–Nd(1)–O(5)	132.75(6)	O(1W)–Nd(1)–O(1)	69.44(6)	O(8)–Nd(1)–O(1)	129.48(6)
O(3)–Nd(1)–O(8)	71.46(6)	O(3)–Nd(1)–O(6)	87.38(6)	O(2)–Nd(1)–O(1)	114.57(6)
O(5)–Nd(1)–O(8)	95.31(7)	O(5)–Nd(1)–O(6)	133.16(6)	O(7)–Nd(1)–O(1)	81.90(6)
O(3)–Nd(1)–O(2)	60.58(5)	O(8)–Nd(1)–O(6)	73.17(6)	O(7)–Nd(1)–O(2)	148.31(6)
O(5)–Nd(1)–O(2)	72.18(6)	O(2)–Nd(1)–O(6)	138.30(6)	O(7)–Nd(1)–O(3)	148.99(6)
O(8)–Nd(1)–O(2)	71.71(7)	O(1W)–Nd(1)–O(6)	139.04(7)	O(7)–Nd(1)–O(8)	119.95(6)
O(3)–Nd(1)–O(1W)	95.19(7)	O(1)–Nd(1)–O(6)	73.10(6)	O(6)–Nd(1)–O(7)	67.12(6)
O(5)–Nd(1)–O(1W)	70.45(7)	O(3)–Nd(1)–O(7)	118.87(5)	O(7)–Nd(1)–O(5)	77.23(6)
O(8)–Nd(1)–O(1W)	145.93(7)	O(5)–Nd(1)–O(7)	71.49(6)	O(7)–Nd(1)–O(6)	70.88(6)
O(2)–Nd(1)–O(1W)	74.45(8)	O(8)–Nd(1)–O(7)	48.61(5)	O(7)–Nd(1)–O(1W)	87.85(8)
O(3)–Nd(1)–O(1)	70.50(6)	O(2)–Nd(1)–O(7)	103.80(7)	O(7)–Nd(1)–O(7)	73.42(7)
O(5)–Nd(1)–O(1)	135.09(7)	O(1W)–Nd(1)–O(7)	140.40(6)	O(1)–Nd(1)–O(7)	138.13(6)
IV					
O(7)–Sm(1)–O(2)	71.41(7)	O(1)–Sm(1)–O(8)	94.08(7)	O(5)–Sm(1)–O(1W)	74.14(9)
O(7)–Sm(1)–O(5)	147.99(6)	O(6)–Sm(1)–O(8)	129.94(7)	O(1)–Sm(1)–O(1W)	71.25(7)
O(2)–Sm(1)–O(5)	138.08(7)	O(1W)–Sm(1)–O(8)	145.30(8)	O(6)–Sm(1)–O(1W)	69.65(7)
O(7)–Sm(1)–O(1)	77.12(7)	O(7)–Sm(1)–O(4)	148.71(6)	O(7)–Sm(1)–O(8)	120.17(7)

Table 2 (*continued*)

Bond long (Å)					
O(2)–Sm(1)–O(1)	132.76(6)	O(2)–Sm(1)–O(4)	86.80(6)	O(2)–Sm(1)–O(8)	73.39(7)
O(5)–Sm(1)–O(1)	72.12(6)	O(5)–Sm(1)–O(4)	61.11(6)	O(5)–Sm(1)–O(8)	71.41(7)
O(7)–Sm(1)–O(6)	81.81(7)	O(1)–Sm(1)–O(4)	133.23(6)	O(5)–Sm(1)–O(7)	104.03(7)
O(2)–Sm(1)–O(6)	73.02(7)	O(6)–Sm(1)–O(4)	70.24(6)	O(1)–Sm(1)–O(7)	71.18(6)
O(5)–Sm(1)–O(6)	114.79(7)	O(1W)–Sm(1)–O(4)	95.07(7)	O(6)–Sm(1)–O(7)	137.58(6)
O(1)–Sm(1)–O(6)	135.88(7)	O(8)–Sm(1)–O(4)	71.85(6)	O(1W)–Sm(1)–O(7)	140.88(7)
O(7)–Sm(1)–O(1W)	87.90(9)	O(7)–Sm(1)–O(7)	73.51(8)	O(8)–Sm(1)–O(7)	48.39(6)
O(2)–Sm(1)–O(1W)	139.42(8)	O(2)–Sm(1)–O(7)	66.68(6)	O(4)–Sm(1)–O(7)	118.73(6)
V					
O(8)–Eu(1)–O(6)	71.54(7)	O(5)–Eu(1)–O(7)	93.24(7)	O(5)–Eu(1)–O(2W)	71.49(7)
O(8)–Eu(1)–O(1)	147.79(6)	O(2)–Eu(1)–O(7)	130.30(7)	O(2)–Eu(1)–O(2W)	69.91(7)
O(6)–Eu(1)–O(1)	138.13(7)	O(2W)–Eu(1)–O(7)	145.13(8)	O(8)–Eu(1)–O(7)	120.21(7)
O(8)–Eu(1)–O(5)	77.12(7)	O(8)–Eu(1)–O(3)	148.51(6)	O(6)–Eu(1)–O(7)	73.54(7)
O(6)–Eu(1)–O(5)	132.30(6)	O(6)–Eu(1)–O(3)	86.66(6)	O(1)–Eu(1)–O(7)	71.33(7)
O(1)–Eu(1)–O(5)	72.06(6)	O(1)–Eu(1)–O(3)	61.43(6)	O(1)–Eu(1)–O(8a)	104.07(7)
O(8)–Eu(1)–O(2)	81.70(7)	O(5)–Eu(1)–O(3)	133.48(6)	O(5)–Eu(1)–O(8a)	70.88(6)
O(6)–Eu(1)–O(2)	73.09(6)	O(2)–Eu(1)–O(3)	70.12(6)	O(2)–Eu(1)–O(8a)	137.37(6)
O(1)–Eu(1)–O(2)	114.92(7)	O(2W)–Eu(1)–O(3)	95.40(8)	O(2W)–Eu(1)–O(8a)	140.78(7)
O(5)–Eu(1)–O(2)	136.38(7)	O(7)–Eu(1)–O(3)	72.18(6)	O(7)–Eu(1)–O(8a)	48.10(6)
O(8)–Eu(1)–O(2W)	87.59(9)	O(8)–Eu(1)–O(8a)	73.68(8)	O(3)–Eu(1)–O(8a)	118.60(6)
O(6)–Eu(1)–O(2W)	139.65(7)	O(6)–Eu(1)–O(8a)	66.38(6)		
VI					
O(2)–Gd(1)–O(4)	71.73(8)	O(9)–Gd(1)–O(3)	71.39(8)	O(5)–Gd(1)–O(1W)	71.89(8)
O(2)–Gd(1)–O(5)	77.10(8)	O(8)–Gd(1)–O(3)	130.49(8)	O(9)–Gd(1)–O(1W)	73.91(9)
O(4)–Gd(1)–O(5)	131.71(7)	O(1W)–Gd(1)–O(3)	144.90(9)	O(8)–Gd(1)–O(1W)	70.19(7)
O(2)–Gd(1)–O(9)	147.70(7)	O(2)–Gd(1)–O(7)	148.47(7)	O(2)–Gd(1)–O(3)	120.09(8)
O(4)–Gd(1)–O(9)	138.00(8)	O(4)–Gd(1)–O(7)	86.63(7)	O(4)–Gd(1)–O(3)	73.37(8)
O(5)–Gd(1)–O(9)	72.11(7)	O(5)–Gd(1)–O(7)	133.61(7)	O(5)–Gd(1)–O(3)	92.42(8)
O(2)–Gd(1)–O(8)	81.81(8)	O(9)–Gd(1)–O(7)	61.52(6)	O(5)–Gd(1)–O(2a)	70.66(7)
O(4)–Gd(1)–O(8)	73.36(7)	O(8)–Gd(1)–O(7)	69.92(7)	O(9)–Gd(1)–O(2a)	104.23(8)
O(5)–Gd(1)–O(8)	137.02(8)	O(1W)–Gd(1)–O(7)	95.42(8)	O(8)–Gd(1)–O(2a)	137.15(7)
O(9)–Gd(1)–O(8)	114.83(7)	O(3)–Gd(1)–O(7)	72.53(7)	O(1W)–Gd(1)–O(2a)	140.98(8)
O(2)–Gd(1)–O(1W)	87.59(10)	O(2)–Gd(1)–O(2a)	73.81(9)	O(3)–Gd(1)–O(2a)	47.70(7)
O(4)–Gd(1)–O(1W)	140.17(8)	O(4)–Gd(1)–O(2a)	65.81(7)	O(7)–Gd(1)–O(2a)	118.39(6)
VII					
O(7)–Tb(1)–O(6)	73.51(11)	O(1)–Tb(1)–O(8)	70.98(9)	O(7)–Tb(1)–O(8)	121.90(12)
O(7)–Tb(1)–O(5)	76.81(9)	O(7)–Tb(1)–O(1W)	85.26(14)	O(6)–Tb(1)–O(8)	73.65(9)
O(6)–Tb(1)–O(5)	128.60(7)	O(6)–Tb(1)–O(1W)	142.35(9)	O(5)–Tb(1)–O(8)	88.31(9)
O(7)–Tb(1)–O(2)	80.46(10)	O(5)–Tb(1)–O(1W)	73.29(8)	O(2)–Tb(1)–O(8)	132.57(9)
O(6)–Tb(1)–O(2)	74.66(7)	O(2)–Tb(1)–O(1W)	71.34(8)	O(2)–Tb(1)–O(3)	69.53(7)
O(5)–Tb(1)–O(2)	139.11(8)	O(1)–Tb(1)–O(1W)	73.08(10)	O(1)–Tb(1)–O(3)	61.46(7)
O(7)–Tb(1)–O(1)	146.10(9)	O(8)–Tb(1)–O(1W)	143.18(10)	O(8)–Tb(1)–O(3)	75.12(8)
O(6)–Tb(1)–O(1)	138.03(9)	O(7)–Tb(1)–O(3)	148.21(8)	O(1W)–Tb(1)–O(3)	94.59(9)
O(5)–Tb(1)–O(1)	72.19(7)	O(6)–Tb(1)–O(3)	88.25(7)	O(5)–Tb(1)–O(3)	133.58(7)
O(2)–Tb(1)–O(1)	115.16(8)				

calculated (mass fraction, the same hereafter, %) for $C_{15}H_{16}O_{11}Ce$ (512.40): C, 35.16; H, 3.15. Found: C, 35.68; H, 3.76. IR data (KBr pellet, cm^{-1}): 3634(w), 3336(br), 2921(w), 2852(w), 1652(s), 1582(s), 1512(s), 1453(s), 1434(s), 1353(m), 1332(m), 1290(w), 1252(w), 1238(w), 1208(s), 1117(w), 1076(w), 1066(w), 1035(w), 954(w), 839(w), 826(m), 741(w), 714(w), 677(w), 619(w), 601(w), 572(w), 531(w), 501(w), 397(w).

*2.2.3. Synthesis of the coordination polymers {[Ln(BDOA)$_{1.5}$(H$_2$O)]·H$_2$O}$_n$ (**II**–**VII**, Ln = Pr(**II**), Nd(**III**), Sm(**IV**), Eu (**V**), Gd (**VI**), Tb(**VII**))*

Coordination polymers **II**–**VII** were prepared by the identical experimental procedures to that of **I** except that cerium nitrate was replaced by praseodymium nitrate, neodymium nitrate, samarium nitrate, europium nitrate, gadolinium nitrate and terbium nitrate, respectively.

For **{[Pr(BDOA)$_{1.5}$(H$_2$O)]·H$_2$O}$_n$ (II)**. Elemental analysis calculated (%) for: $C_{15}H_{16}O_{11}Pr$ (513.19): C, 34.78; H, 3.10. Found: C, 35.11; H, 3.14. IR data (KBr pellet, cm^{-1}): 3632(w), 3493(w), 3423(br), 2918(w), 1653(s), 1581(s), 1512(s), 1454(s), 1434(s), 1353(m), 1333(m), 1290(w), 1252(w), 1239(w), 1208(s), 1116(w), 1076(m), 1034(m), 954(w), 839(w), 826(m), 742(w), 713(w), 669(w), 620(w), 602(w), 572(w), 533(w), 391(w), 376(w).

For **{[Nd(BDOA)$_{1.5}$(H$_2$O)]·H$_2$O}$_n$ (III)**. Elemental analysis calculated (%) for $C_{15}H_{16}O_{11}Nd$ (516.52): C, 34.88; H, 3.12. Found: C, 35.27; H, 3.14. IR data (KBr pellet, cm^{-1}): 3631(w), 3496(w), 3316(br), 2933(w), 1655(s), 1581(s), 1512(s), 1454(s), 1434(s), 1353(m), 1333(m), 1290(w), 1252(w), 1237(w), 1206(s), 1117(w), 1064(m), 1035(m), 955(w), 934(w), 839(w), 826(m), 742(w), 714(w), 687(w), 620(w), 602(w), 572(w), 533(w), 519(w), 502(w), 396(w), 378(w).

For **{[Sm(BDOA)$_{1.5}$(H$_2$O)]·H$_2$O}$_n$ (IV)**. Elemental analysis calculated (%) for $C_{15}H_{16}O_{11}Sm$ (522.63): C, 34.47; H, 3.08. Found: C, 35.02; H, 3.16. IR data (KBr pellet, cm^{-1}): 3551 (w), 3478(w), 3415(w), 3238(w), 1639(s), 1618(s), 1511(s), 1454(w), 1427(s), 1353(w), 1334(w), 1190(w), 1206(w), 1118(w), 1065(w), 1033(w), 826(w), 621(s), 623(w), 601(w), 576(w), 529(w), 517(w), 499(w), 479(s), 405(s).

For **{[Eu(BDOA)$_{1.5}$(H$_2$O)]·H$_2$O}$_n$ (V)**. Elemental analysis calculated (%) for $C_{15}H_{16}O_{11}Eu$ (524.24): C, 34.22; H, 3.01. Found: C, 34.37; H, 3.08. IR data (KBr pellet, cm^{-1}): 3630 (br), 3496 (w), 3297 (s), 2933(s), 1660(s), 1585(s), 1512(s), 1456(w), 1435(s), 1354(w), 1336(w), 1291(w), 1208(s), 1118(w), 1064(w), 958(w), 936(w), 836(w), 745(w), 621(w), 571(w), 535(w), 503(w), 397(s), 376(s).

Table 3
Hydrogen-bond lengths (Å) and angles (°) for coordination polymers **I**–**VII**.

D–H···A	d(D–H)	d(H···A)	d(D···A)	∠(DHA)
I				
O(1W)–H(1WA)···O(1)	0.85	1.969	2.728	148.21
O(1W)–H(1WB)···O(2W)	0.85	1.967	2.752	153.26
O(2W)–H(2WA)···O(4)	0.85	2.211	2.987	151.86
II				
O(1W)–H1(WB)···O(2)	0.85	2.09	2.723(3)	131.0
O(1W)–H1(WA)···O(2W)	0.85	2.20	2.743(3)	121.2
O(2W)–H2(WA)···O(4)	0.85	2.25	2.976(3)	142.9
III				
O(1W)–H(1WA)···O(2)	0.85	1.98	2.719(3)	144.5
O(1W)–H(1WB)···O(2W)	0.85	1.90	2.741(3)	168.4
O(2W)–H(2WB)···O(4)	0.85	2.48	2.977(3)	117.8
IV				
O(1W)–H(1WA)···O(5)	0.85	2.08	2.710(3)	130.2
O(1W)–H(1WB)···O(2W)	0.85	1.93	2.757(3)	165.4
O(1W)–H(1WB)···O(3)	0.85	2.13	2.959(3)	166.6
V				
O(1W)–H(1WB)···O(4)	0.85	2.17	2.955(3)	154.0
O(2W)–H(2WA)···O(1W)	0.85	1.92	2.752(3)	165.2
O(2W)–H(2WB)···O(1)	0.85	1.95	2.709(3)	148.7
VI				
O(1W)–H(1WA)···O(5)	0.85	2.08	2.710(3)	130.2
O(1W)–H(1WB)···O(2W)	0.85	1.93	2.757(3)	165.4
O(1W)–H(1WB)···O(3)	0.85	2.13	2.959(3)	166.6
VII				
O(1W)–H(1WB)···O(4)	0.85	2.17	2.955(3)	154.0
O(2W)–H(2WA)···O(1W)	0.85	1.92	2.752(3)	165.2
O(2W)– H(2WB)···O(1)	0.85	1.95	2.709(3)	148.7

For **{[Gd(BDOA)$_{1.5}$(H$_2$O)]·H$_2$O}$_n$ (VI)**. Elemental analysis calculated (%) for $C_{15}H_{16}O_{11}Gd$ (529.53): C, 34.05; H, 3.02. Found: C, 34.02; H, 3.04. IR data (KBr pellet, cm^{-1}): 3629 (br), 3495 (w), 3296 (s), 2932(s), 1660(s), 1584(s), 1512(s), 1456(w), 1433(s), 1354(w), 1333(w), 1291(w), 1208(s), 1120(w), 1064(w), 958(w), 937(w), 836(w), 745(w), 622(w), 571(w), 535(w), 504(w), 397(s), 376(w).

For **{[Tb(BDOA)$_{1.5}$(H$_2$O)]·H$_2$O}$_n$ (VII)**. Elemental analysis calculated (%) for $C_{15}H_{16}O_{11}Tb$ (531.20): C, 33.92; H, 3.04. Found: C, 34.02; H, 3.14. IR data (KBr pellet, cm^{-1}): 3662 (s), 3494(s), 2967(w), 2932(s), 1673(s), 1589(s), 1513(s), 1457(w), 1434(s), 1356(w), 1296(w), 1239(s), 1209(w), 1119(w), 1065(w), 1033(w), 827(w), 752(w), 714(w), 609(w), 566(w), 537(w), 524(w), 506(w), 397(s), 379(s).

2.2.4. Crystallographic data collection and refinement

Single-crystal diffraction data **I**–**VII** were collected Suitable single crystals of the coordination polymers on a Bruker Smart CCD X-ray single-crystal diffractometer with graphite monochromated MoKα-radiation (λ = 0.71073 Å) at 296(2) K. All independent reflections were collected in a range of 1.77–25.00° for **I**, 1.78–25.00 for **II**, 2.16–25.00 for **III**, 1.78–25.00 for **IV**, 1.79–25.00 for **V**, 1.79–25.00 for **VI**, and 1.79–25.00 for **VII** (determined in the subsequent refinement). Multi-scan empirical absorption corrections were applied to the data using the SADABS. The crystal structure was solved by direct methods and Fourier synthesis. Positional and thermal parameters were refined by the full-matrix least-squares method on F^2 using the SHELXTL software package. The final least-square cycle of refinement gave, R_1 = 0.0201, wR_2 = 0.0501 for **I**, R_1 = 0.0174, wR_2 = 0.0425 for **II**, R_1 = 0.0171, wR_2 = 0.0424 for **III**, R_1 = 0.0174, wR_2 = 0.0458 for **IV**, R_1 = 0.0156, wR_2 = 0.0418 for **V**, R_1 = 0.0180, wR_2 = 0.0485 for **VI**, and R_1 = 0.0170, wR_2 = 0.0440 for **VII**. The weighting scheme, $w = 1/[\sigma^2(F_0^2) + (0.0180P)^2 + 0.62P]$ for **I**, $w = 1/[\sigma^2(F_0^2) + (0.0187P)^2 + 1.29P]$ for **II**, $w = 1/[\sigma^2(F_0^2) + (0.0211P)^2 + 1.63P]$ for **III**, $w = 1/[\sigma^2(F_0^2) + (0.0313P)^2 + 0.25P]$ for **IV**, $w = 1/[\sigma^2(F_0^2) + (0.2000)^2 + 0.00P]$ for **V**, $w = 1/[\sigma^2(F_0^2) + (0.0252)^2 + 0.00P]$ for **VI**, and $w = 1/[\sigma^2(F_0^2) + (0.0192)^2 + 2.12P]$ for **VII**, Where $P = (F_0^2 + 2F_c^2)/3$. A summary of the key crystallographic information is given in Table 1. Selected bond lengths and band angles for the coordination polymers **I**–**VII** are listed in Table 2. Hydrogen-bond lengths (Å) and angles (°) for **I**–**VII** are listed in Table 3.

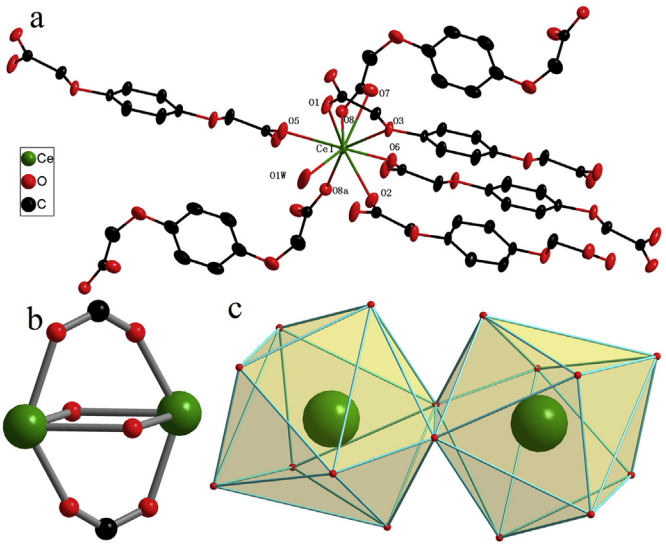

Fig. 1. (a) Diagram showing the coordination environments for Ce(III) centers in **I** (30% probability displacement ellipsoids); (b) The connection mode of Ce(III) ions in cavate 10-membered cage $Ce_2O_2(OCO)_2$; (c) Polyhedrons for the two crystallographically independent Ce(III) ions.

3. Results and discussion

3.1. The IR spectra of the coordination polymers

Coordination polymers are insoluble in common solvents such as CH_3COCH_3, CH_3CH_2OH, and $CH_3CH_2OCH_3CH_2$, but they are slight soluble in CH_3OH, DMSO, and DMF. The structures of the coordination polymers are identified by satisfactory elemental analysis as well as FT-IR and X-ray analyses. High yield of the products indicate that the title coordination polymers are thermodynamically stable under the reaction conditions. The FT-IR spectra of the six as-synthesized coordination polymers are similar. The strong and broad absorption bands in the ranges of 3456–3318 cm^{-1} and 917–907 cm^{-1} in **I**–**VII** are assigned to the stretching vibrations of ν(O–H) in water molecules in coordination and lattice forms [56–58].

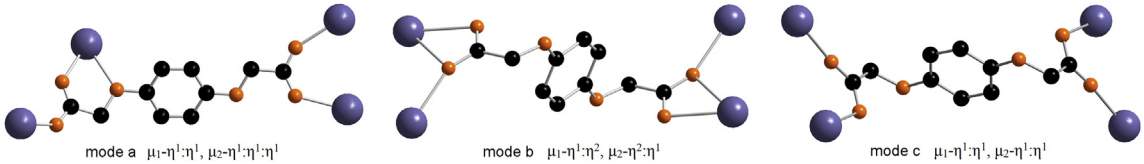

Scheme 1. Coordination modes of BDOA^{2-} ligand in coordination polymers **I**–**VII**.

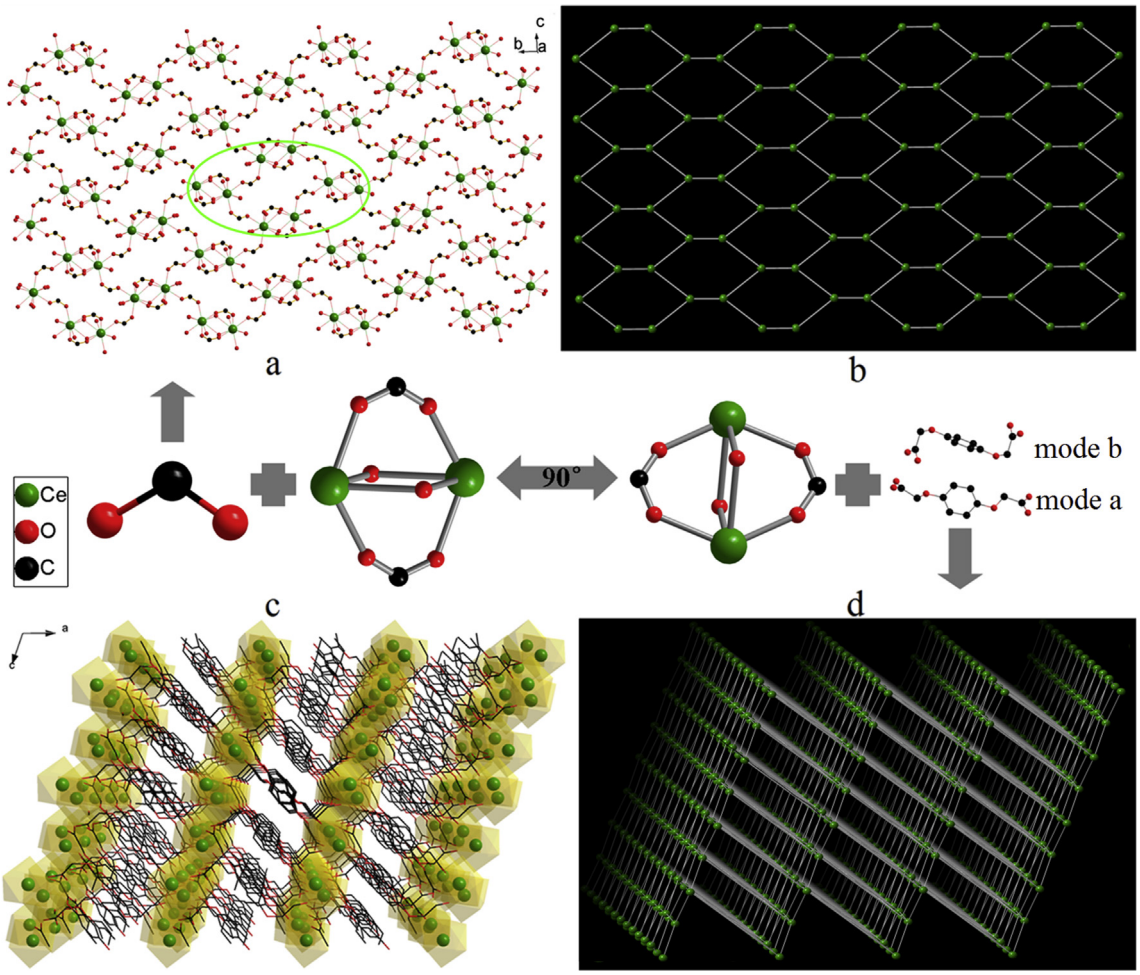

Fig. 2. (a) Diagram showing the 2D framework connected through O–C–O (μ_1-η^1:η^1) linkers between the adjacent cavate 10-membered cages ($Ce_2O_2(OCO)_2$) in **I**; (b) View of the 2D (6, 6) sheet in **I**; (c) Diagram showing the 1D-cavity-containing 3D architecture in **I**; (d) Topological graph of **I** showing the 3D architecture connected through $BDOA^{2-}$ linkers between the adjacent 2D layers in **I**. All hydrogen atoms are omitted for clarity.

The features present in the range of 1076–1064 cm^{-1} can be ascribed to the stretching vibrations of ν(C–O–C) in BDOA ligands. Another features in the region of 1673–1511 cm^{-1} and 1457–1332 cm^{-1} may be ascribed to the asymmetric (COO^-) and symmetric (COO^-) stretching of carboxyl groups of BDOA ligands in **I**–**VII**. The values of $\Delta[\nu_{as} - \nu_s]$ are about 199–216 and 157–180 cm^{-1}, which indicate that the carboxyl groups are coordinated with the metal ions *via* both bidentate-chelating and mono-chelating modes [59,60]. The sharp peaks of δ_{O-C-O} vibration in plane emerge in the range of 660–760 cm^{-1}. The absorption bands at 1064 cm^{-1} is attributed to stretching vibration of the Ar–O–CH_2. The absorption at about 826 cm^{-1} is related to the *p*-disubstituted benzene stretching vibration [61]. The absence of the characteristic bands around 1700 cm^{-1} indicates that the H_2BDOA ligands are completely deprotonated in the form of $BDOA^{2-}$ anions upon reaction with the metal ions [62,63]. The same conclusions are also supported by the results obtained from X-ray diffraction measurements.

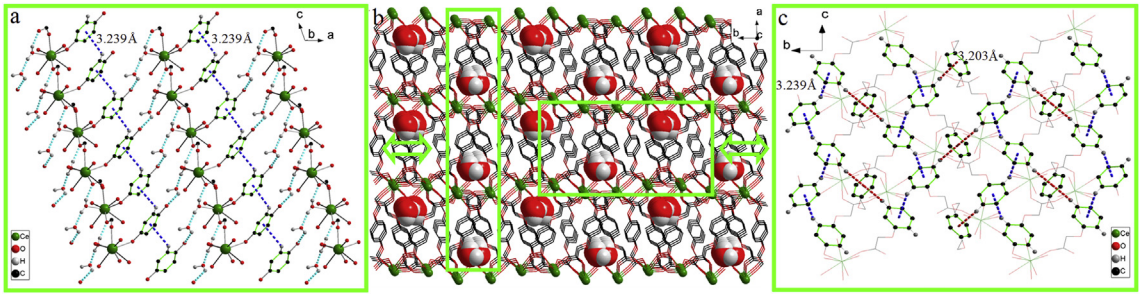

Fig. 3. (a) Hydrogen bonds (light green dotted line) and C–H···π interactions (blue dotted line) in the 2D layer in **I**; (b) Diagram showing the embedded guest water molecules in the 3D architecture of **I**; (c) Two kinds of C–H···π interactions (indicated as blue dotted line and red dotted line, respectively) between the adjacent benzene rings of $BDOA^{2-}$ ligands in **I**. (For interpretation of the references to color in this figure legend, the reader is referred to the web version of this article.)

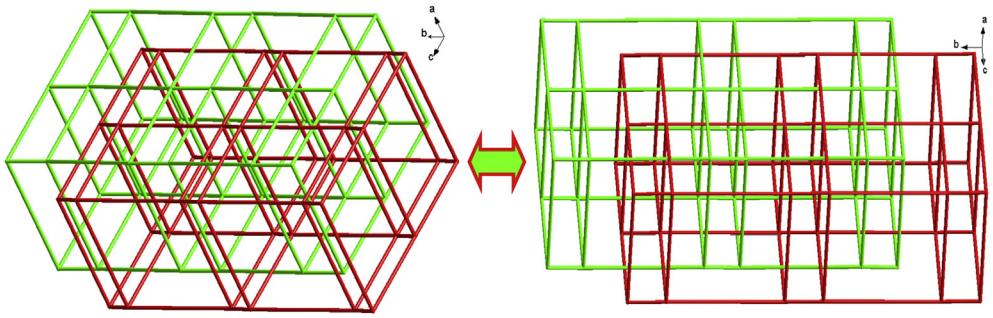

Fig. 4. Schematic representation of the interpenetrated network topology of **I**.

3.2. Structural description of the coordination polymers

The $BDOA^{2-}$ ligands display three different types of coordination modes, which are exhibited in Scheme 1. Namely, mode *a* adopts the fashion of μ_1-η^1:η^1, μ_2-η^1:η^1:η^1, while mode *b* and mode *c* take the fashions of μ_1-η^1:η^2, μ_2-η^2:η^1 and μ_1-η^1:η^1, μ_2-η^1:η^1, respectively. The single-crystal analyses reveal that coordination polymers **I**–**VII** are isomorphous and that **I**–**VI** are isostructural, crystallizing in monoclinic space group *P*21/*c*. The prominent feature of their structure is a cavity-containing 3D framework consisting of cavate 10-membered cages ($Ln_2O_2(OCO)_2$) bridged by $BDOA^{2-}$ ligands. As a representative example, the fabrication of 3D structure of coordination polymer $\{[Ce(BDOA)_{1.5}(H_2O)]\cdot H_2O\}_n$ (**I**) is described here in detail. The 9-coordinated Ce(III) center is surrounded by eight oxygen atoms from four molecules of the ligand with mode *a*, two with mode *b*, and one water molecule to furnish a bicapped trigonal antiprism geometry (Fig. 1a and c). Namely, Ce(III) is nine-coordinated with nine oxygen donors containing one O atom (O_w) coming from the terminal water, one O atom coming from ether oxygen atoms (O_{ether}) and others belong to carboxylic oxygen atoms ($O_{carboxyl}$). The average distance of Ce—$O_{carboxyl}$ is 2.529 Å, which is significantly shorter than that of Ce—O_w bonds (2.532 Å). The bond length data in the present work are consistent with those in previous work covering lanthanide coordination polymers [64,65].

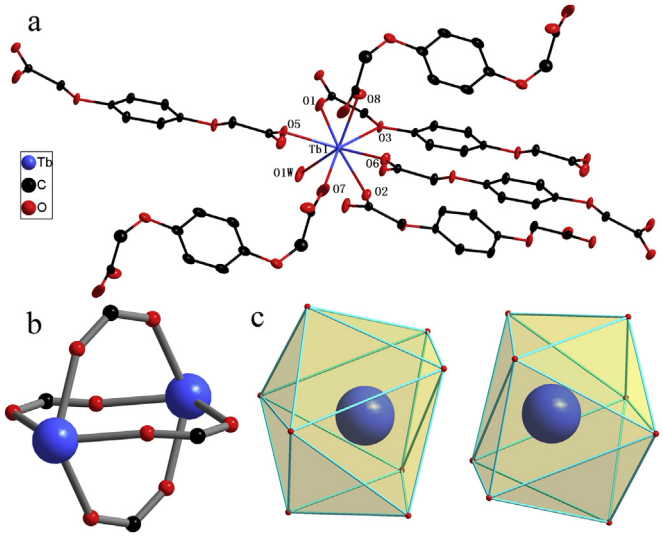

Fig. 5. (a) Diagram showing the coordination environment for Tb(III) centers in **VII** (30% probability displacement ellipsoids); (b) The connection mode of Tb(III) ions in cavate 14-membered cage $Tb_2(OCO)_4$; (c) Polyhedron for the two crystallographically independent Tb(III) ions in a binuclear unit. All hydrogen atoms and lattice-water molecules are omitted for clarity.

The adjacent two crystallographically equivalent Ce(III) ions (Ce···Ce) are bridged by two oxygen atoms (i.e. O(8)) in μ_2-η^2 fashion and two carboxy groups (i.e. O(5)—C(10)—O(6)) in μ_1-η^1:η^1 fashion with the nonbonding distance of 4.166 Å to form a cavate 10-membered cage ($Ce_2O_2(OCO)_2$) which serves as the subunit in the architecture (see Fig. 1b). In terms of the framework of coordination polymer **I**, every four neighboring 10-membered cages are linked into approximate hexagon grids through the carboxy groups in μ_1-η^1:η^1, μ_2-η^1:η^1:η^1 (mode *a*) fashion and are further connected into an infinite 2D (6, 6) sheet, as illustrated in Fig. 2a and b. In the hexagon grid, the interior angles ($\angle$Ce···Ce···Ce) are 144.309°, 121.636° and 89.590°, the length of sides (Ce···Ce) are 4.166 Å and 6.339 Å, respectively. Furthermore, acting as connectors, the $BDOA^{2-}$ ligands are in anticonformation such that the carboxy groups at each end of the benzene rings point in opposite direction. The twist angles of 50.119°, 28.935° (for mode *a*) and 80.486°(for mode *b*) between corresponding benzene ring and carboxy groups are observed, respectively, which define that the 2D (6, 6) sheet presents an undulating 2D framework. Findings indicate that coordination polymer **I** displays a cavity-containing (with an approximate dimension of 6.339 × 12.521 $Å^2$) 3D architecture constructed based on the subunit of cavate 10-membered cages ($Ce_2O_2(OCO)_2$) between the 2D (6, 6) sheet *via* two types linkers of the $BDOA^{2-}$ ligands in mode *a* (μ_1-η^1:η^1, μ_2-η^1:η^1:η^1) and mode *b* (μ_1-η^1:η^2, μ_2-η^2:η^1), as shown in Fig. 2c and d.

It is noteworthy that there exist two types of 2D layers along *b* and *a* axis in the ordered 3D skeleton. Hydrogen bonds (i.e. O(1W)—H(1WA)···O(1), 2.728 Å, 148.21°, O(1W)—H(1WB)···O(2W), 2.752 Å, 153.26°, and O(2W)—H(2WA)···O(4), 2.987 Å, 151.86°) stabilize the embedded guest water molecules in the 2D corrugated layer (see Fig. 3a and Table 3). Structural characterizations and thermogravimetric analyses have also manifested the presence of embedded guest water molecules in these coordination polymers (Fig. 3b) [66]. Simultaneously, C—H···π interactions occur between the adjacent benzene rings of $BDOA^{2-}$ ligands (i.e. C(6)—H(6)···π = 3.239 Å and C(3)—H(3)···π = 3.203 Å) which reinforce the structure effectively, as depicted in Fig. 3a and c. Thus, these nonbonding weak interactions aforementioned actually drive the

Table 4
Comparison of the corresponding distances (average) for coordination polymers **I**–**VII**.

	I	II	III	IV	V	VI	VII
Ln—Ow (Å)	2.532	2.507	2.496	2.456	2.441	2.4303	2.417
Ln—$O_{carboxyl}$ (Å)	2.529	2.507	2.497	2.476	2.463	2.422	2.370
Ln…Ln (Å)	4.166	4.144	4.136	4.127	4.127	4.139	4.220
Ln—O_{ether} (Å)	2.707	2.683	2.675	2.647	2.632	2.622	2.615
Dimensions of the cavities ($Å^2$)	79.367	78.665	78.606	78.016	77.501	77.265	76.617

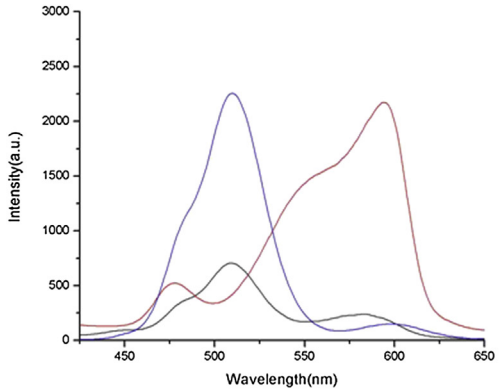
Intensity(a.u.)
Wavelength(nm)

a

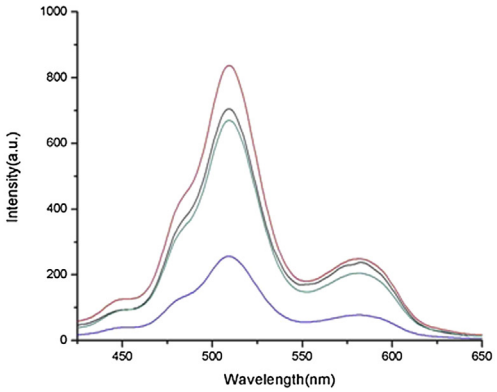
Intensity(a.u.)
Wavelength(nm)

b

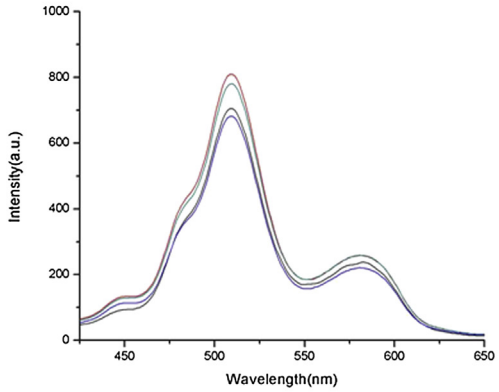
Intensity(a.u.)
Wavelength(nm)

c

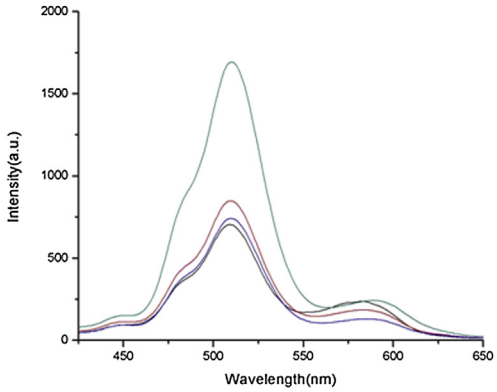
Intensity(a.u.)
Wavelength(nm)

d

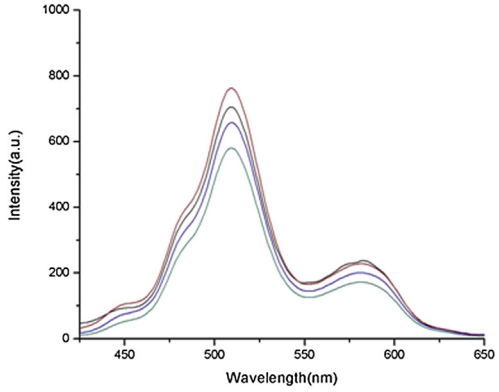
Intensity(a.u.)
Wavelength(nm)

e

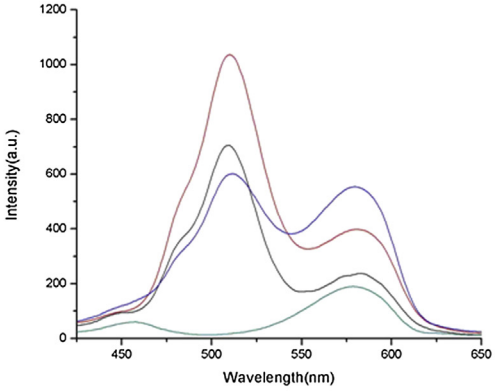
Intensity(a.u.)
Wavelength(nm)

f

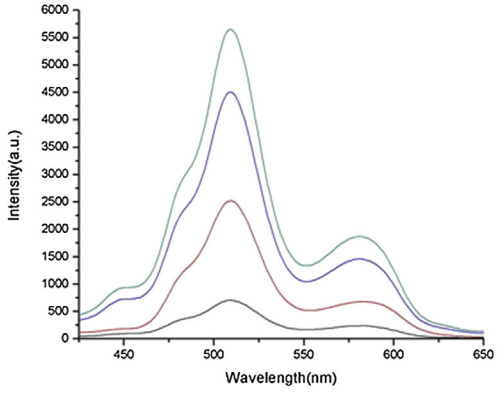
Intensity(a.u.)
Wavelength(nm)

g

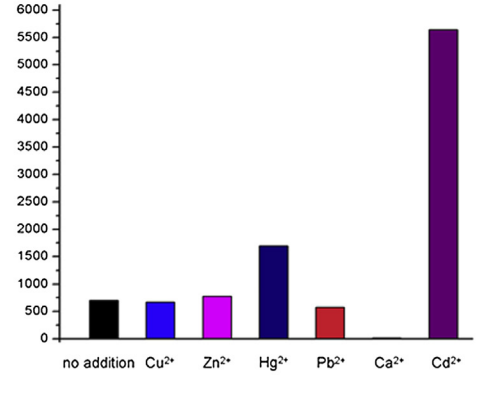
no addition
Cu2+
Zn2+
Hg2+
Pb2+
Ca2+
Cd2+

h

self-assembly of the 3D architecture. As a result, these structural features may help us to understand how the bulk water plays an important role to stabilize the conformation of coordination polymer in the self-assembly process as well as diversified non-covalent weak interactions. Interestingly, the as-synthesized coordination polymer **I** features a peculiar interpenetrated 3D topological structure (see Fig. 4).

3.3. Structure comparison of the coordination polymers

As the results aforementioned, **I**–**VI** and **VII** were synthesized under similar hydrothermal conditions, yet the coordination environment around Tb(III) in **VII** consists of four molecules of the ligand with mode *a* (μ_1-η^1:η^1, μ_2-η^1:η^1:η^1), two with mode *c* (μ_1-η^1:η^1, μ_2-η^1:η^1), and one water molecule which is different with those around Ln(III)(Ln = Ce(**I**), Pr(**II**), Nd(**III**), Sm(**IV**), Eu(**V**), and Gd(**VI**)). Namely, Tb(III) ion is eight-coordinated with O_8 donor set containing six $BDOA^{2-}$ ligands (O(1), O(2), O(3), O(5), O(6), O(7), and O(8)) and one terminal water molecule (O(1W)) to complete the coordination geometry. The Tb–O bond lengths range from 2.281 to 2.616 Å (average 2.400 Å), which are in agreement with those reported earlier of other Tb(III) coordination polymers [67,68]. By comparison, in the structures of **I**–**VI**, the Ln(III) centers adopt nine-coordinated (Ln1O9) coordination environments and present bicapped trigonal antiprism geometries, whereas Tb(III) ion takes eight-coordinated (Tb1O8) coordination environment and demonstrates a distorted dodecahedron configuration in **VII**, which is mainly due to the obvious decrease in cationic radii of Tb(III) by comparison to those of Ce(III), Pr(III), Nd(III), Sm(III), Eu(III), and Gd(III) to connect with fewer metallic nodes, which cause the reduction of the coordination number (see Fig. 5). The most obvious structural difference between **I**–**VI** and **VII** is as follow: The adjacent two Tb(III) ions (Tb···Tb) are bridged by four carboxy groups (i.e. O(5)–C(10)–O(6)) and (O(7)–C(11)–O(8)) in μ_2-η^1:η^1 fashion with the nonbonding distance of 4.220 Å to form a cavate 14-membered cage ($Tb_2(OCO)_4$) differing from those cages in **I**–**VI** which serves as the subunit in the 3D architecture (see Fig. 5b). In addition to structural difference of the cages, features of the approximate hexagon grid and infinite 2D (6, 6) sheet in **VII** are similar to those in **I**–**VI**. Although structures of **III** and **V** had been reported, these coordination polymers were also obtained independently by us by simply tuning the Ln(III)/H_2BDOA ratio, with different solvent system, different temperature and shorter reaction time. Furthermore, the lanthanide contraction, experiments on luminescent probers, as well as thermogravimetric analyses are systematically studied, which did not appear elsewhere.

3.4. Lanthanide contraction

As discussed above, coordination polymers **I**–**VI** are isomorphous and isostructural. Simultaneously, **I**–**VI** exhibit obvious lanthanide contraction effect, which is evidenced by their crystal lattice constants. As shown in Table 4, the average distances of Ln–O_w, Ln–$O_{carboxyl}$ in **I**–**VI** decrease slightly following the order of Ce, Pr, Nd, Sm, Eu, and Gd, consistent with lanthanide contraction, which may be ascribed to the crystal field contractions of the rare earth ions lacking of spherical symmetry [69,70].

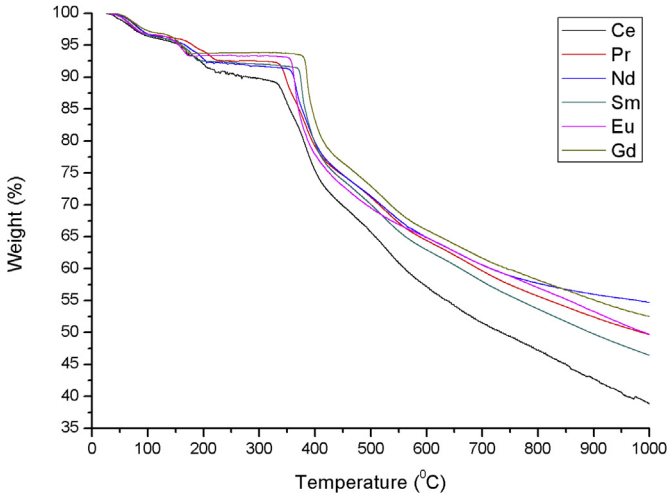

Fig. 7. The TG curves for coordination polymers **I**–**VI**.

The similar trend is occurred in Ln···Ln separations, which decrease from 4.166 to 4.139 Å. As a result, dimensions of the cavities in the 3D architectures in **I**–**VI** decrease progressively and the densities increase by degrees along with lanthanide contraction (from 79.367 to 77.265 $Å^2$ and from 1.968 to 2.098 Mg/m^3, respectively). The 4f electrons of lanthanide in the coordination polymers are shielded by the outershell $5s^2$ and $5p^6$ orbitals and therefore are scarcely available for covalent interaction with the organic ligands. As a result, electrostatic interactions are dominant in the Ln(III) coordination polymers, and the geometries of the coordination polymers are determined by steric factors rather than electrostatic effects [71].

3.5. Luminescent properties

To examine the possibility of modification of the luminescent properties through cations exchange, the solid sample of **I**, **II**, **V**, and **VII** were immersed in water (10^{-4} M) containing various metal cations to generate solutions at room temperature. Noteworthy, the emission intensity of **I** (Fig. 6) increases significantly upon adding 1–3 Cd^{2+} ($Cd(CH_3COO)_2$) equivalents with respect to **I**. The highest peak at 524 nm is nearly quintuple, ninefold and twelvefold as intense as the corresponding band in the solution without Cd^{2+}. To further understanding of this phenomenon, the same experiments were performed for the introduction of Cu^{2+} ($Cu(CH_3COO)_2$), Zn^{2+} ($Zn(CH_3COO)_2$), Hg^{2+} ($HgSO_4$), Pb^{2+} ($Pb(CH_3COO)_2$), and Ca^{2+} ($CaCl_2$) into the system. Interestingly, the luminescence quenched when adding 3 equivalents of Ca^{2+} to the solution of **I**. The emission intensity at 524 nm of the coordination polymer is two and a half times enhanced at the presence of 3×10^{-4} M Hg^{2+} ($HgSO_4$) in contrast to **I**. Comparatively, the emission intensities at 524 nm did not change obviously at the introductions of Cu^{2+}, Zn^{2+}, and Pb^{2+} ions with respect to the coordination polymer. These results suggest that coordination polymer **I** shows selectivity toward Ca^{2+} and Cd^{2+} and it can be considered as selective luminescent probes for these metals. The mechanism accounting for the luminescent feature of the coordination polymers along

Fig. 6. (a–g): Emission spectra of **I** in water (10^{-4} M) at RT (excited at 348 nm) in the presence of Cu^{2+}, Zn^{2+}, Hg^{2+}, Pb^{2+}, Ca^{2+}, and Cd^{2+} ions with respect to **I**; a: black, **I** (10^{-4} M); red, H_2BDOA; blue, $Ce(NO_3)_3{\cdot}6H_2O$ (10^{-4} M); b: Cu^{2+}; c: Zn^{2+}; d: Hg^{2+}; e: Pb^{2+}; f: Ca^{2+}, and g: Cd^{2+} (black, no addition; red, 1 equiv; blue, 2 equiv; green, 3 equiv); (h): Luminescent intensity of **I** at 524 nm at room temperature upon the addition of 3 equiv.Cu^{2+}, Zn^{2+}, Hg^{2+}, Pb^{2+}, Ca^{2+}, and Cd^{2+}. (For interpretation of the references to color in this figure legend, the reader is referred to the web version of this article.)

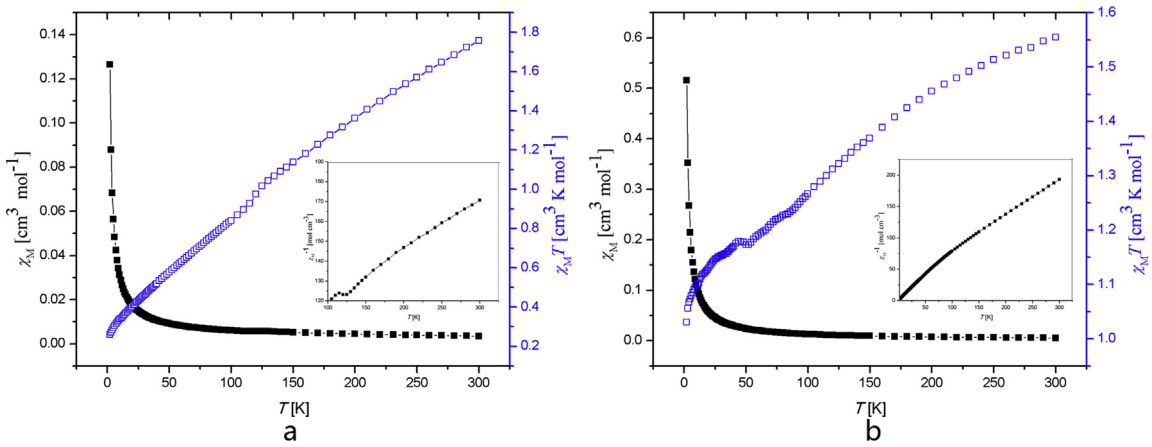

Fig. 8. (a) Thermal variation of χ_M and $\chi_M T$ for coordination polymer **I**. Insert: Plot of thermal variation of χ_M^{-1} for coordination polymer **I**; (b) Thermal variation of χ_M and $\chi_M T$ for coordination polymer **III**. Insert: Plot of thermal variation of χ_M^{-1} for coordination polymer **III**.

with its dependence on the co-existing metal ions is still under investigation.

Moreover, emission spectra of **II** (excited at 323 nm), **V** (excited at 321 nm), and **VII** (excited at 322 nm) in the presence of Cu^{2+}, Hg^{2+}, Zn^{2+}, Cd^{2+}, Mn^{2+}, and Ca^{2+} ions with respect to original coordination polymers are depicted in Fig. S1, Fig. S2, and Fig. S3, respectively. Except for **II**, the luminescent intensity enhances with Cd^{2+}. The others luminescent intensities of **II**, **V**, and **VII** are either unchanged or smaller changed.

3.6. Thermogravimetric analysis

Thermogravimetric analysis of **I**–**VI** performed in the N_2 stream from room temperature to 1000 °C shows that all the coordination polymers decompose in three steps and their TG curves are almost similar (see Fig. 7). The first stage weight losses of as-synthesized coordination polymers **I**–**VI** (3.96%, 3.66%, 3.68%, 3.63%, 3.45%, and 3.32%, respectively) take place covering the temperature ranges of 25–115, 25–116, 25–117, 25–118, 25–118, and 25–120 °C corresponding to the destruction of one lattice water molecule, which are close to relevant calculated weight loss of 3.52%, 3.51%, 3.49%, 3.46%, 3.45%, and 3.43% and consistent with the crystal structure analysis. The second weight loss stage has a decomposition temperature range of 134–229, 143–231, 147–251, 133–194, 122–172, and 129–174 °C, with a weight loss of 5.04%, 3.58%, 3.63%, 3.80%, 3.27%, and 3.07%, respectively. This can be assigned to the loss of one coordinated water molecule that calculated weight loss is 3.52%, 3.51%, 3.49%, 3.46%, 3.45%, and 3.43%, respectively. A stable plateau emerges around 247–319, 251–318, 229–340, 209–355, 192–334, and 182–360 °C in the TG curves, followed by the third stage weight loss at 324, 326, 342, 362, 344, and 369 °C owing to the decomposition of $BDOA^{2-}$ ligands, giving the final residual products of Ln_2O_3 (Pr_6O_{11} for **II**). The remnants of coordination polymers **I**–**VI** after the third stage are 39.01%(**I**), 46.66%(**II**), 47.93%(**III**), 46.67%(**IV**), 49.66%(**V**), and 47.46%(**VI**), which suggests that they do not decompose completely under the experimental temperature (calculated values of Ln_2O_3 for coordination polymers **I**–**VI** are 32.02% (Ce_2O_3), 33.17% (Pr_6O_{11}), 32.57% (Nd_2O_3), 33.36% (Sm_2O_3), 33.57% (Eu_2O_3), and 34.54% (Gd_2O_3)). Moreover, it is worthy to note that the dehydration and decomposition temperatures of coordination polymers **I**–**VI** rise with the increase of the atomic number of lanthanide elements, corresponding to the lanthanide contraction in association with the decrease of Ln–O_w, Ln–$O_{carboxyl}$, Ln···Ln distances and dimensions of the cavities (see Table 4) [72–74].

3.7. Magnetic properties

Variable-temperature magnetic susceptibility of $\{[Ce(BDOA)_{1.5}(H_2O)]\cdot H_2O\}_n$ (**I**) and $\{[Nd(BDOA)_{1.5}(H_2O)]\cdot H_2O\}_n$ (**III**) are measured in the 2–300 K temperature range. The variation of the inverse of the magnetic susceptibility, χ_M^{-1} and $\chi_M T$ of **I** and **III** are shown in Fig. 8a and b. For **I**, the $\chi_M T$ value at 300 K is 1.754 cm^3 K mol^{-1} (3.745 μB), which is higher than the expected value (0.1378 cm^3 K mol^{-1}, 1.050 μB) of an isolated spin-only Ce(III) ions ($S = 1/2$, $g = 6/7$). the $\chi_M T$ value of $\{[Ce(BDOA)_{1.5}(H_2O)]\cdot H_2O\}_n$ decrease very slowly until it reaches a minimum of 0.2514 cm^3 K mol^{-1} about 2 K. This behavior indicates a dominant antiferromagnetic interaction between the Ce(III) ions in the structures. The χ_M^{-1} versus T plot of **I** is in correspondence with the Curie–Weiss constant determined in the range of 2–300 K with $C = 1.970$ cm^3 K mol^{-1} and $\theta = -96.593$ K.

For **III**, the magnetic behavior is similar with that of **I**. the $\chi_M T$ value at 300 K is 0.5992 cm^3 K mol^{-1} (2.189 μB), which is closed to the expected value (0.4959 cm^3 K mol^{-1}, 1.991 μB) of an isolated spin-only Nd(III) ions ($S = 3/2$, $g = 8/11$). With the decrease of temperature, the $\chi_M T$ value decrease very slowly until it reaches 0.1866 cm^3 K mol^{-1} about 52 K, and the χ_M^{-1} versus T plot of **III** is in correspondence with Curie–Weiss constant determined in the range of 2–300 K with $C = 1.680$ cm^3 K mol^{-1} and $\theta = -29.614$ K. Then the $\chi_M T$ increases to 0.1947 cm^3 K mol^{-1} at 45 K, finally, the $\chi_M T$ value decrease rapidly a minimum of 0.0306 cm^3 K mol^{-1}. This indicates that the magnetic interaction of Nd(III) is antiferromagnetic, and it is also in accordance with the literature.

4. Conclusion

Summarily, seven lanthanide-containing coordination polymers based on the flexible $BDOA^{2-}$ ligands were successfully synthesized under hydrothermal conditions. The ligands exhibit three different coordination modes in the coordination polymers, and result in two different structural types, which demonstrate the lanthanide contraction effect in **I**–**VI**. The Ln(III) centers adopt 9-coordinated coordination environment to furnish bicapped trigonal antiprism geometries in **I**–**VI**, while it takes 8-coordinated coordination environment to present a distorted dodecahedron configuration in **VII**. Coordination polymers **I**–**VI** are isomorphous and isostructural, containing the subunit of cavate 10-membered cages ($Ln_2O_2(OCO)_2$), while **VII** possesses the subunit of cavate 14-membered cages ($Tb_2(OCO)_4$), based on which to assemble into 3D porous architectures *via* $BDOA^{2-}$ ligands, hydrogen bonds

together with C–H···π interactions. Moreover, the thermal stability of the coordination polymers was evaluated by thermogravimetric analysis, suggesting that the dehydration and decomposition temperatures of coordination polymers **I** to **VI** are approximately rising with lanthanide contraction. Besides, coordination polymer **I** and **III** present antiferromagnetic behaviors. Particularly, luminescent studies suggest the efficient energy transfer from $BDOA^{2-}$ ligands to the corresponding Ln(III) ions, exhibiting the typical intense emissions of Ln(III) ions in the visible region and therefore the lanthanide coordination polymers display good selectivity towards some certain metal ions such as Ca^{2+} and Cd^{2+}. The results suggest that some of these coordination polymers may be potential multifunctional materials in selective luminescent probes and magnetism.

Acknowledgments

This research is financially supported by the Natural Science Foundation of Henan Province of China (No. 13A150056, 2012B150005, 122102210174 and 12B150004).

Appendix A. Supplementary data

Supplementary data related to this article can be found at http://dx.doi.org/10.1016/j.dyepig.2014.01.032.

References

[1] Xu J, Su W-P, Hong M-C. A series of lanthanide secondary building units based metal-organic frameworks constructed by organic pyridine-2,6-dicarboxylate and inorganic sulfate. Cryst Growth Des 2010;11(1):337–46.
[2] Thomas D, Christian S, Nathalie A, Marrot J, Gérard F. MIL-103, a 3-D lanthanide-based metal organic framework with large one-dimensional tunnels and a high surface area. J Am Chem Soc 2005;127(37):12788–9.
[3] Shi F-N, Cunha-Silva L, SáFerreira RA, Mafra L, Trindade T, Carlos LD, et al. Interconvertable modular framework and layered lanthanide(III)-etidronic acid coordination polymers. J Am Chem Soc 2008;130(1):150–67.
[4] Deng H, Qiu Y-C, Li Y-H, Liu Z-H, Olivier G. Supramolecular isomers of lanthanides (III): synthesis, crystal structures and luminescent properties. Inorg Chim Acta 2009;362(6):1797–804.
[5] Yang L-R, Wu L-Z, Zhang H-M, Song S, Liu L, Li M-X. Synthesis, structure and luminescent recognition properties of cerium (IV) coordination polymers based on pyridine-2,6-dicarboxylic acid. Dye Pigment 2013;99:257–67.
[6] Chandrasekhar V, Hossain S, Das S, Biswas S, Sutter JP. Rhombus-shaped tetranuclear [Ln4] complexes [Ln = Dy (III) and Ho (III)]: synthesis, structure, and SMM behavior. Inorg Chem 2013;52(11):6346–53.
[7] Wan Y-H, Zhang L-P, Jin L-P, Gao S, Lu S-Z. High-dimensional architectures from the self-assembly of lanthanide ions with benzenedicarboxylates and 1,10-phenanthroline. Inorg Chem 2003;42(16):4985–94.
[8] Gao H-L, Yi L, Zhao B, Zhao X-Q, Cheng P, Liao D-Z, et al. Synthesis and characterization of metal-organic frameworks based on 4-hydroxypyridine-2,6-dicarboxylic acid and pyridine-2,6-dicarboxylic acid ligands. Inorg Chem 2006;45(15):5980–8.
[9] Prasad TK, Rajasekharan MV. A novel water octamer in $Ce(dipic)_2(H_2O)_3\cdot 4H_2O$: crystallographic, thermal, and theoretical studies. Cryst Growth Des 2006;6(2):488–91.
[10] Lee JY, Farha OK, Roberts J, Scheidt KA, Nguyen ST, Hupp JT. Metal-organic framework materials as catalysts. Chem Soc Rev 2009;38(5):1450–9.
[11] Li J-R, Kuppler RJ, Zhou H-C. Selective gas adsorption and separation in metal-organic frameworks. Chem Soc Rev 2009;38(5):1477–504.
[12] Ke F, Yuan Y-P, Qiu L-G, Shen Y-H, Xie A-J, Zhu J-F, et al. Facile fabrication of magnetic metal-organic framework nanocomposites for potential targeted drug delivery. J Mater Chem 2011;21(11):3843–8.
[13] Ma M-L, Ji C, Zang S-Q. Syntheses, structures, tunable emission and white light emitting eu^{3+} and tb^{3+} doped lanthanide metal-organic framework materials. Dalton Trans 2013;42:10579–86.
[14] Chai X-C, Sun Y-Q, Lei R, Chen Y-P, Zhang S, Cao Y-N, et al. A series of lanthanide frameworks with a flexible ligand, N,N′-diacetic acid imidazolium, in different coordination modes. Cryst Growth Des 2009;10(2):658–68.
[15] Zhu T-Y, Ikarashi K, Ishigaki T, Uematsu K, Toda K, Okawa H, et al. Structure and luminescence of sodium and lanthanide (III) coordination polymers with pyridine-2,6-dicarboxylic acid. Inorg Chim Acta 2009;362(10):3407–14.
[16] Wu J-Y, Yeh TT, Wen YS, Twu J, Lu KL. Unusual robust luminescent porous frameworks self-assembled from lanthanide ions and 2,2′-bipyridine-4,4′-dicarboxylate. Cryst Growth Des 2006;6(2):467–73.
[17] Chantal BC, Jeannette DG, Auguste F, Joël J, Jean CT. Synthesis, crystal structures and properties of three new lanthanide 2,6-pyridinedicarboxylate complexes with zero-dimensional structure. Inorg Chim Acta 2008;361(9):2909–17.
[18] Hu D-X, Luo F, Che Y-X, Zheng J-M. Construction of lanthanide metal-organic frameworks by flexible aliphatic dicarboxylate ligands plus a rigid m-phthalic acid ligand. Cryst Growth Des 2007;7(9):1733–7.
[19] Halim M, Tremblay MS, Jockusch S, Turro NJ, Sames D. Transposing molecular fluorescent switches into the near-IR: development of luminogenic reporter substrates for redox metabolism. J Am Chem Soc 2007;129(25):7704–5.
[20] Allendorf MD, Bauer CA, Bhakta RK, Houk RJT. Luminescent metal-organic frameworks. Chem Soc Rev 2009;38(5):1330–52.
[21] Wang P, Ma J-P, Dong Y-B, Huang R-Q. Tunable luminescent lanthanide coordination polymers based on reversible solid-state ion-exchange monitored by ion-dependent photoinduced emission spectra. J Am Chem Soc 2007;129(35):10620–1.
[22] Xu J, Cheng J-W, Su W-P, Hong M-C. Effect of lanthanide contraction on crystal structures of three-dimensional lanthanide based metal-organic frameworks with thiophene-2,5-dicarboxylate and oxalate. Cryst Growth Des 2011;11(6):2294–301.
[23] Silva P, Silva LC, Silva NJO, Rocha J, AlmeidaPaz FA. Metal-organic frameworks assembled from erbium tetramers and 2,5-pyridinedicarboxylic acid. Cryst Growth Des 2013;13(6):2607–17.
[24] Zhao B, Cheng P, Dai Y, Cheng C, Liao D-Z, Yan S-P, et al. A nanotubular 3D coordination polymer based on a 3d-4f heterometallic assembly. Angew Chem Int Ed 2003;42(8):934–6.
[25] Zhao B, Chen X-Y, Cheng P, Liao D-Z, Yan S-P, Jiang Z-H. Coordination polymers containing 1D channels as selective luminescent probes. J Am Chem Soc 2004;126(47):15394–5.
[26] Tanase S, Gallego PM, Gelder R, Fu W-T. Synthesis, crystal structure and photophysical properties of europium (III) and terbium (III) complexes with pyridine-2,6-dicarboxamide. Inorg Chim Acta 2007;360(1):102–8.
[27] Mahata P, Ramya KV, Natarajan S. Synthesis, structure and optical properties of rare-earth benzene carboxylates. Dalton Trans 2007;36:4017–26.
[28] Dong Y-B, Wang P, Ma J-P, Zhao X-X, Wang H-Y, Tang B, et al. Coordination-driven nanosized lanthanide "molecular lantern" with tunable luminescent properties. J Am Chem Soc 2007;129(16):4872–3.
[29] Cui Y-J, Yue Y-F, Qian G-D, Chen B-L. Luminescent functional metal-organic frameworks. Chem Rev 2011;112(2):1126–62.
[30] Horcajada P, Gref R, Baati T, Allan PK, Maurin G, Couvreur P, et al. Metal-organic frameworks in biomedicine. Chem Rev 2011;112(2):1232–68.
[31] Sun L-X, Qi Y, Wang Y-M, Che Y-X, Zheng J-M. A variety of novel complexes constructed from biphenyl-3,3′,4,4′-tetracarboxylate and flexible bis (imidazole) ligands. CrystEngComm 2010;12(5):1540–7.
[32] Campbell K, Kuehl CJ, Ferguson MJ, Stang PJ, Tykwinski RR. Coordination-driven self-assembly: solids with bidirectional porosity. J Am Chem Soc 2002;124(25):7266–7.
[33] Li S-L, Lan Y-Q, Ma J-F, Yang J, Wei G-H, Zhang L-P, et al. Structures and luminescent properties of seven coordination polymers of zinc (II) and cadmium (II) with 3,3′,4,4′-benzophenone tetracarboxylate anion and bis (imidazole). Cryst Growth Des 2008;8(2):675–84.
[34] Li S-L, Lan Y-Q, Ma J-C, Ma J-F, Su Z-M. Metal-organic frameworks based on different benzimidazole derivatives: effect of length and substituent groups of the ligands on the structures. Cryst Growth Des 2010;10(3):1161–70.
[35] Yaghi OM, O'Keeffe M, Ockwig NW, Chae HK, Eddaoudi M, Reticular JK. Reticular synthesis and the design of new materials. Nature 2003;423(6941):705–14.
[36] Hasegawa S, Horike S, Matsuda R, Furukawa S, Mochizuki K, Kinoshita Y, et al. Three-dimensional porous coordination polymer functionalized with amide groups based on tridentate ligand: selective sorption and catalysis. J Am Chem Soc 2007;129(9):2607–14.
[37] Chen B-L, Zhao X-B, Putkham A, Hong K-L, Lobkovsky EB, Hurtado EJ, et al. Surface interactions and quantum kinetic molecular sieving for H2 and D2 adsorption on a mixed metal-organic framework material. J Am Chem Soc 2008;130(20):6411–23.
[38] Grosu OG, Lönnecke P, Dumitrescu LS, Hawkins EH, Anorg Z. Coordination polymers of the heterotopic 1,4-phenylenebis (oxy) diacetic acid ligand: cadmium(II) complexes. Allg Chem 2011;637(12):1722–7.
[39] Gong Y-N, Liu C-B, Ding Y, Xiong Z-Q, Xiong L-M. Syntheses and structures of copper benzene-1,4-dioxydiacetate complexes with 4,4′-bipyridine and 1,10-phenanthroline. J Coord Chem 2010;63(11):1865–72.
[40] Yang Y, Jiang G-Q, Li Y-Z, Bai J-F, Pan Y, You X-Z. Synthesis, structures and properties of alkaline earth metal benzene-1,4-dioxylacetates with three-dimensional hybrid networks. Inorg Chim Acta 2006;359(10):3257–63.
[41] Gao S, Liu J-W, Huo L-H, Xu Y-M, Zhao H. A two-dimensional Cd(II) coordination polymer:$[Cd(1,4\text{-}BDOA)(1,10\text{-}phen)]\cdot H_2O$ with strong blue fluorescent emission constructed by benzene-1,4-dioxydiacetate ligand. Inorg Chem Commun 2005;8(4):361–4.
[42] Li X-Y, Liu C-B, Che G-B, Wang X-C, Li C-X, Yan Y-S, et al. Four metal-organic networks based on benzene-1,4-dioxyacetic acid and dipyrido [3,2-a: 2′,3′-c] phenazine ligand. Inorg Chim Acta 2010;363(7):1359–66.
[43] Hong X-L, Li Y-Z, Hu H-M, Pan Y, Bai J-F, You X-Z. Synthesis, structure, luminescence, and water induced reversible crystal-to-amorphous transformation properties of lanthanide (III) benzene-1,4-dioxylacetates with a three-dimensional framework. Cryst Growth Des 2006;6(6):1221–6.

[44] Sabbatini N, Guardigli M, Lehn JM. Luminescent lanthanide complexes as photochemical supramolecular devices. Coord Chem Rev 1993;123(1):201–28.
[45] Wang M-X, Long L-S, Huang R-B, Zheng L-S. Influence of halide ions on the chirality and luminescent property of ionothermally synthesized lanthanide-based metal-organic frameworks. Chem Commun 2011;47:9834–96.
[46] Sato T, Higuchi M. A vapoluminescent Eu-based metallo-supramolecular polymer. Chem Commun 2012;48:4947–9.
[47] Cui Y-J, Xu H, Yue Y-F, Guo Z-Y, Yu J-C, Chen Z-X, et al. A luminescent mixed-lanthanide metal-organic framework thermometer. J Am Chem Soc 2012;134(9):3979–82.
[48] Milon J, Daniel MC, Kaiba A, Guionneau P, Brandès S, Sutter JP. Nanoporous magnets of chiral and racemic [{Mn (HL)} 2Mn {Mo (CN)$_7$}$_2$] with switchable ordering temperatures (TC = 85 K ↔ 106 K) driven by H_2O sorption (L = N,N-dimethylalaninol). J Am Chem Soc 2007;129(45):13872–8.
[49] Kurmoo M. Magnetic metal-organic frameworks. Chem Soc Rev 2009;38(5):1353–79.
[50] Milon J, Guionneau P, Duhayon C, Sutter JP. [K_2Mn_5 {Mo (CN)$_7$}$_3$]: an open framework magnet with four Tc conversions orchestrated by guests and thermal history. New J Chem 2011;35(6):1211–8.
[51] Zhao X-Q, Liu X-H, Li J-J, Zhao B. Syntheses, structures, photoluminescence and magnetic properties of four-connected lanthanide-tricarboxylate coordination polymers. CrystEngComm 2013;15:3308–17.
[52] Yang L-R, Song S, Zhang W, Zhang H-M, Bu Z-W, Ren T-G. Synthesis, structure and luminescent properties of neodymium (III) coordination polymers with 2,3-pyrazinedicarboxylic acid. Synth Met 2011;161(9):647–54.
[53] Yang L-R, Song S, Zhang W, Zhang H-M, Bu Z-W, Ren T-G. Synthesis, structure and luminescent properties of 3D lanthanide (La (III), Ce (III)) coordination polymers possessing 1D nanosized cavities based on pyridine-2,6-dicarboxylic acid. Synth Met 2011;161(15):1500–8.
[54] Yang L-R, Song S, Shao C-Y, Zhang W, Zhang H-M, Bu Z-W, et al. Synthesis, structure and luminescent properties of two-dimensional lanthanum (III) porous coordination polymer based on pyridine-2,6-dicarboxylic acid. Synth Met 2011;161(11):925–30.
[55] Yang L-R, Song S, Zhang H-M, Wu L-Z. Synthesis, characterization and thermal decomposition kinetics as well as evaluation of luminescent properties of several 3D lanthanide coordination polymers as selective luminescent probes of metal ions. Synth Met 2012;162(21):1775–88.
[56] Tang R-R, Gu G-L, Zhao Q. Synthesis of Eu (III) and Tb (III) complexes with novel pyridine dicarboxamide derivatives and their luminescence properties. Spectrochim Acta Part A 2008;71(2):371–6.
[57] Yang L-R, Song S, Zhang W, Zhang H-M, Bu Z-W, Ren T-G. Synthesis, structure of 3D lanthanide (La(III), Pr(III)) nanoporous coordination polymers containing 1D channels as selective luminescent probes of Pb^{2+}, Ca^{2+} and Cd^{2+} ions. Synth Met 2011;161(21):2230–40.
[58] Infrared NK, Raman. Infrared and Raman spectra of inorganic and coordination chemistry. New York: Wiley; 1997.
[59] Tancrez N, Feuvrie C, Ledoux I, Zyss J, Toupet L, Bozec HL, et al. Lanthanide complexes for second order nonlinear optics: evidence for the direct contribution of f electrons to the quadratic hyperpolarizability 1. J Am Chem Soc 2005;127(39):13474–5.
[60] Shi F-N, Silva LC, Trindade T. Three-dimensional lanthanide-organic frameworks based on di-, tetra-, and hexameric clusters. Cryst Growth Des 2009;9(5):2098–109.
[61] Li X-F, Han Z-B, Cheng X-N, Chen X-M. Studies on the radii dependent lanthanide self-assembly coordination behaviors of a flexible dicarboxylate ligand. Inorg Chem Commun 2006;9(11):1091–5.
[62] Aghabozorg H, Moghimi A, Manteghi F, Ranjbar M. A nine-coordinated ZrIV complex and a self-assembling system obtained from a proton transfer compound containing 2,6-pyridinedicarboxylate and 2,6-pyridinediammonium; synthesis and X-ray crystal structure. Z Anorg Allg Chem 2005;631(5):909–13.
[63] Liu M-S, Yu Q-Y, Cai Y-P, Su C-Y, Lin X-M, Zhou X-X, et al. One-, two-, and three-dimensional lanthanide complexes constructed from pyridine-2,6-dicarboxylic acid and oxalic acid ligands. Cryst Growth Des 2008;8(11):4083–91.
[64] Yu L-Q, Huang R-D, Xu Y-Q, Liu T-F, Chu W, Hu C-W. Syntheses, structures and properties of novel 3D lanthanide metal-organic frameworks with paddle-wheel building blocks. Inorg Chim Acta 2008;361(7):2115–22.
[65] Weng Z-H, Liu D-C, Chen Z-L, Zou H-H, Qin S-N, Liang F-P. Two types of lanthanide coordinatio n polymers of (2,3-f)-pyrazino(1,10)phenanthroline-2,3-dicarboxylic acid: syntheses, structures, and properties. Cryst Growth Des 2009;9(9):4163–70.
[66] Feng X, Zhao J-S, Liu B, Wang L-Y, Ng S, Zhang G, et al. A series of lanthanide-organic frameworks based on 2-propyl-1H-imidazole-4,5-dicarboxylate and oxalate: syntheses, structure s, luminescence, and magnetic properties. Cryst Growth Des 2010;10(3):1399–408.
[67] Yang J, Song S-Y, Ma J-F, Liu Y-Y, Yu Z-T. Syntheses, structures, photoluminescence, and gas adsorption of rare earth-organic frameworks based on a flexible tricarboxylate. Cryst Growth Des 2011;11(12):5469–74.
[68] Luo Y-H, Yue F-X, Yu X-Y, Chen X, Zhang H. A series of entangled Zn II/Cd II coordination polymers constructed from 1,3,5-benzenetricarboxylate acid and flexible triazole ligands. CrystEngComm 2013;15(40):8116–24.
[69] Yao J, Deng B, Sherry LJ, McFarland AD, Ellis DE, Duyne RPV, et al. Syntheses, structure, some band gaps, and electronic structures of CsLnZnTe3 (Ln = La, Pr, Nd, Sm, Gd, Tb, Dy, Ho, Er, Tm, Y). Inorg Chem 2004;43(24):7735–40.
[70] Sun Y-Q, Yang G-Y. Organic-inorganic hybrid materials constructed from inorganic lanthanide sulfate skeletons and organic 4,5-imidazoledicarboxylic acid. Dalton Trans 2007;34:3771–81.
[71] Armelao L, Quici S, Barigelletti F, Accorsi G, Bottaro G, Cavazzini M, et al. Design of luminescent lanthanide complexes: from molecules to highly efficient photo-emitting materials. Coord Chem Rev 2010;254(5):487–505.
[72] Wang C, Wang Z, Gu F, Guo G. Five novel metal-organic framework constructed by lanthanide metals and 2,2′-bipyridine-6,6′-dicarboxylate: hydrothermal synthesis, crystal structure, and thermal properties. J Mol Struct 2010;979(1):92–100.
[73] Guo X-F, Feng M-L, Xie Z-L, Li J-R, Huang X-Y. The first examples of lanthanide selenite-carboxylate compounds: syntheses, crystal structures and properties. Dalton Trans 2008;23:3101–6.
[74] Chen X-L, Yao Y-J, Hu H-M, Chen S-H, Fu F, Han Z-X, et al. A series of metal-organic frameworks constructed with 2,2′-bipyridine-3,3′-dicarboxylate: syntheses, structures, and physical properties. Inorg Chim Acta 2011;67(11):364–6.